Drug Design, Development and Therapy

Dovepress
open access to scientific and medical research

Open Access Full Text Article

ORIGINAL RESEARCH

Optimized formulation of multivesicular liposomes loaded with oleanolic acid enhanced anticancer effect in vitro

This article was published in the following Dove Press journal:
Drug Design, Development and Therapy
27 March 2017
Number of times this article has been viewed

Yunlong Wang[1,*]
Yuling Luo[1,*]
Chunhong Li[1]
Xiaoqin Zhang[1]
Chao Pi[1]
Lu Yu[2]
Shurong Wang[1]
Zhirong Zhong[1]

[1]Department of Pharmaceutical Sciences, School of Pharmacy, [2]Department of Chemistry, The Institute of Basic Medical Sciences, Southwest Medical University, Luzhou, Sichuan, People's Republic of China

*These authors contributed equally to this work

Abstract: Invasion and metastasis are the main causes leading to the death of patients with hepatocellular carcinoma (HCC). Multivesicular liposomes loaded with oleanolic acid (OA-MVLs) have been well demonstrated to suppress survival, growth and angiogenesis of HCC cells. Emerging evidence demonstrates that OA was able to suppress the invasion of HCC cells by down-regulating myocyte enhancer factor-2. We hypothesized that the optimized OA-MVLs could inhibit the migration and invasion of HCC cells. In this study, we utilized central composite design and response surface methodology to assess the influence of some parameters on particle size and encapsulation efficiency and obtain the optimized formulation of OA-MVLs. Subsequently, the human HCC cell lines SMMC-7721 and HepG2 were treated with different doses of OA-MVLs and OA, respectively. Cellular survival, adhesion, migration and invasion in vitro were evaluated. We found that the optimized OA-MVLs significantly decreased the ability of HCC cells to adhere, migrate and invade in vitro. Furthermore, OA-MVLs significantly inhibited the survival of HCC cells at 160 μmol/L but showed no obvious inhibition effect on the cell vitality of normal liver cells. Our findings indicate that OA-MVLs did inhibit the cell survival, adhesion, invasion and metastasis of HCC cells in vitro. Although the involved mechanisms are still unclear, our findings can contribute to a better development of a preventive and therapeutic strategy for human HCC.

Keywords: oleanolic acid, multivesicular liposomes, central composite design, adhesion, invasion, migration

Introduction

Hepatocellular carcinoma (HCC), a highly aggressive malignant liver tumor, is one of the most prevalent types of cancers worldwide and one of the most common causes of cancer-associated mortality.[1,2] Currently, surgical resection and transplantation are the most effective treatment approaches for HCC.[3] However, patients with HCC usually have a poor prognosis. Postoperative metastasis and recurrence are common, and the recurrence rate within 2 years in patients who have undergone tumor resection remains >50%.[4] Uncontrolled tumor metastasis, frequent intrahepatic spread and extrahepatic metastases are the primary causes for the poor prognosis in HCC.[5] Therefore, preventing invasion and metastasis is critical for effective clinical treatment against HCC.

Oleanolic acid (OA), a pentacyclic triterpenoid found in a variety of plant species, exhibits antitumor capacity on a variety of cancer types,[6–8] including HCC, through multiple mechanisms. Moreover, OA displayed no significant cytotoxicity to normal tissue-derived cells, ensuring its application in clinical treatment. More importantly, OA also

Correspondence: Zhirong Zhong
Department of Pharmaceutical Sciences, School of Pharmacy, Southwest Medical University, 3-319 Zhongshan Road, Luzhou, Sichuan 646000, People's Republic of China
Tel/fax +86 139 8279 6280
Email zhongzhirong@126.com

submit your manuscript | www.dovepress.com
Dovepress
http://dx.doi.org/10.2147/DDDT.S128795

possessed anti-metastasis capacity on some types of cancers. A group found that OA treatment inhibited lung metastasis of B16F10 melanoma cells in a mice model.[9] Osteosarcoma cells also showed a reduced incidence of lung metastasis when exposed to an OA derivative.[10] Others have reported that OA can also suppress the invasiveness and the process from epithelial-to-mesenchymal transition (EMT) of HCC cells.[11] Thus, OA is worth being developed for anti-invasion drugs in HCC treatment. But it has been known that OA possesses significant first-pass effect of liver and undergoes low dissolution in gastrointestinal tract because of the poor water solubility.[12,13] Therefore, it is essential to develop a novel dosage form for OA to improve the treatment efficiency for HCC.

In a previous study, we have developed a novel dosage form of multivesicular liposomes (MVLs) for OA to overcome its poor solubility, prolong therapeutic drug levels in the blood and enhance the antitumor effect on HCC. All the results showed that OA-MVLs significantly enhanced cell growth inhibition against human HCC HepG2 cells in vitro and potentiated the antitumor efficacy in mice bearing HCC in vivo.[14] However, the action of OA-MVLs on HCC adhesion, invasion and metastasis has not been investigated yet. Moreover, as we know, the formation of OA-MVLs will be affected by many variable factors, such as characteristics of solution, lipid composition and process parameters, and other factors also have an impact on drug release from OA-MVLs. Response surface methodology (RSM) is a collection of statistical and mathematical methods that is useful for modeling and analyzing engineering problems.[15] The main objective of RSM is to optimize the response surface that is influenced by various process parameters. RSM also quantifies the relationship between the controllable input parameters and the obtained response surfaces.[15,16] Therefore, in this study, we used a central composite design (CCD) and RSM to examine the main and/or interactive effects of a factorial combination of ratio of cholesterol and soybean lecithin, total lipids and drug and triolein and soybean lecithin on the particle size and encapsulation efficiency of OA-MVLs.

With these backgrounds mentioned earlier, we hypothesized that the optimized formulation of OA-MVLs could suppress the metastatic process of HCC, which, in turn, would underscore the therapeutic potential of OA-MVLs in HCC prevention and cure. Accordingly, this study was designed to optimize the formulation of OA-MVLs and test the hypothesis by examining the cell survivability of L-02, HepG2 and SMMC-7721 cells and investigating the cell adhesion, migration and invasion inhibition against HepG2 and SMMC-7721 cells.

Materials and methods

Materials

OA was purchased from Keyang (Luzhou, China). The standard of OA was provided by Must BioTechnology Company (Chengdu, China; purity >98%). Triolein was supplied by Aladdin Chemistry Company (Shanghai, China). Soybean lecithin was obtained from Tywei Pharmaceutical Company (Shanghai, China; purity >90%). Cholesterol, Tween-80 and polyvinyl alcohol were supplied by Kelong Chemical Reagent Factory (Chengdu, China). Stearic acid was acquired from National Medicine Group Chemical Company (Beijing, China). Matrigel matrix was purchased from BD Biosciences (San Jose, CA, USA).

Roswell Park Memorial Institute (RPMI) 1640 culture medium, Dulbecco's Modified Eagle's Medium (DMEM), penicillin and streptomycin were purchased from Hammer Flew Biochemical Company (Beijing, China). Fetal bovine serum (FBS) was obtained from TianHang Biotechnology Company (Huzhou, China). 3-(4,5 dimethylthiozol-2-yl)-2,5-diphenyl-tetrazolium bromide (MTT) and dimethyl sulfoxide (DMSO) were purchased from Sigma. Paraformaldehyde was provided by Jinshan Chemical Company (Chengdu, China).

Cell lines and cell culture

HCC cell lines SMMC-7721 and HepG2 and human normal liver cell line L-02 were obtained from Shanghai Cell Institute, China Academy of Sciences, and preserved in our laboratory. SMMC-7721 and HepG2 cells were cultured in DMEM supplemented with 10% FBS and L-02 cells in RPMI 1640 with 10% FBS at 37°C and 5% CO_2. All procedures of human cells were conducted in accordance with the principles and protocol approved by the Human Cell Ethics Committee of Southwest Medical University.

Preparation of OA-MVLs

OA (molecular weight [MW] 456.7) was dissolved to a concentration of 10 mmol/L by DMSO, stored at −20°C and diluted in culture medium that was prepared with saline to the required concentration, then filtered using 0.22 μm filter and stored at 4°C for further use. The solvent, the same concentration of DMSO (0.25%) with OA solution, was used as control, which was proved to be toxicity free by a series of preliminary experiments.

OA-MVLs were prepared by a double-emulsion method. The first step is to prepare the water-in-oil (W/O) solution by emulsifying sucrose solution (7%) with mixture of soybean lecithin, cholesterol, triolein, stearic acid and OA dissolved in chloroform/diethyl ether (1:1, v/v), in which the shearing

was at 33.75 m/s for 2 min. Next, the preformed W/O solution was further emulsified with an aqueous solution containing glucose (4%), Tween-80 (2%) and polyvinyl alcohol (0.3%) to get a water-in-oil-in-water (W/O/W) double emulsion. Finally, the W/O/W solution was subjected to a rotary evaporation to remove chloroform and diethyl ether, which resulted in the formation of OA-MVLs. The final products were stored at 4°C for further use.

Formulation optimization of OA-MVLs

CCD is an experimental design for the optimization of pharmaceutical dosage forms. It was developed by Box and Wilson using RSM.[17] It is the most commonly used optimization method with the multi-advantages of fewer test, high precision and predictability. It can be used in the nonlinear fitting of the mathematical model. RSM guides the plan of the experiments and the parsimonious analysis of data to gain a maximum amount of information most efficiently.[18] Therefore, in this study based on the preliminary experiments, three variables that significantly influenced the encapsulation efficiency (Y_1) and particle size (Y_2) were taken as the main factors, ie, ratio of cholesterol and soybean lecithin (X_1, w/w), total lipids and drug (X_2, w/w) and triolein and soybean lecithin (X_3, w/w).

In general, the total number of CCD points is $N=2^k+2k+1$, in which k represents the number of factors to be studied. In this study, three variables were considered. Thus, the design points are $N=2^3+2\times3+1=15$. Accordingly, a three-factor CCD requires 15 experimental points, each of which being a result of different formulations. In order to estimate the pure experimental uncertainty of CCD, it is important to measure repeatedly the response function to the conditions determined by the central points. In this case, five repeated experiments were performed. The nonlinear quadratic model generated by the design is of the form: $Y=b_0+b_1X_1+b_2X_2+b_3X_3+b_4X_1X_2+b_5X_1X_3+b_6X_2X_3+b_7X_1^2+b_8X_2^2+b_9X_3^2$, where Y is the measured response associated with each factor-level combination; b_0 is the free term of the regression equation; b_1–b_9 are the regression coefficients and X_1, X_2 and X_3 are the coded independent factors. The constant and the regression coefficients were calculated using the statistical package Statistica (vision 10.0; Statsoft Inc., Tulsa, OK, USA). In order to check the validity of the model, correlation coefficients were taken as the criteria for validation.

In this experiment, we used high-performance liquid chromatography (HPLC) analysis method to detect the encapsulation efficiency (Y_1). Briefly, chromatographic separation was performed on a reverse-phase C18 column (4.6×250 mm, 5 µm particle size, made in China) with a guard column (Phenomenex C18, 4.0×3.0 mm) maintained at 30°C. The mobile phase was a mixture of methanol, water, acetic acid and triethylamine (90:10:0.04:0.02, v/v) at a flow rate of 0.8 mL/min. It was monitored at 210 nm, and the injection volume was 20 µL. Moreover, the chromatographic conditions were validated through specificity, linearity, limit of detection, precision, accuracy and extraction recovery. Meanwhile, to determine the particle size (Y_2), we took high-resolution photographs by the microscope and analyzed the average size, using Image-pro plus 6.0 professional image processing software.

Cytotoxicity assay

To evaluate whether the optimized formulation of OA-MVLs would show in vitro toxicity to normal cells and anticancer efficacy to cancer cells, MTT assay was conducted in HCC cell lines SMMC-7721 and HepG2 and human normal liver cell line L-02. The cells in logarithmic growth phase were seeded onto 96-well plates at a density of 5×10^4 cells per well. After reaching ~80% confluence, the cells were, respectively, treated for 24 h with 100 µL of OA solution or OA-MVLs at different concentrations of 40, 80, 120, 160, 200, 240, 280, 300, 320 and 350 µmol/L, taking the solvent of DMSO (0.25%) as control. After incubation, MTT (5 mg/mL) was added into each well, and the cells were incubated for 4 h at 37°C in the dark. Then, the culture medium was discarded and 150 µL of DMSO was loaded in each well. The optical density (OD) was measured in an ELISA reader (BenchMark; Bio-Rad, CA, USA) at 490 nm (reference filter 570 nm). Five reduplicate wells were measured at each concentration (n=5), and every experiment was performed at least three times. The cell viability was assessed as follows: cell viability (%) $=(A_{treatment}-A_{background})/(A_{control}-A_{background})\times100$, in which the control cells were not subjected to treatment and the background well had no cells in it.

Cell adhesion assay

Cell matrix adhesion assay was performed with both HepG2 and SMMC-7721 cells. Briefly, the 96-well plates were pre-coated with 40 µL Matrigel at 4°C overnight and blocked for 2 h at 37°C with 2% bovine serum albumin (BSA) before seeding cells. Both HepG2 and SMMC-7721 cells were pre-treated separately with OA and OA-MVLs (80, 160 and 240 µmol/L) for 24 h at 37°C. A cell suspension containing 5×10^5 cells/mL was prepared in serum-free medium, and 100 µL of it was added to the inside of each well, in which the untreated cells were taken as control. Cells were allowed to attach for 2 h at 37°C. Subsequently, the non-adherent cells were removed by gentle washing three times with phosphate-buffered saline (PBS). For qualitative

observation, the cells were fixed in 4% paraformaldehyde for 30 min and stained with 0.1% crystal violet dye for 25 min. For quantitative detection, 20 μL of MTT was added and the plates were cultured for another 4 h. The supernatant was replaced by 150 μL DMSO. The plates were shaken for 10 min to ensure the purple crystals were completely dissolved. Then, absorbance of each well was measured on an ELISA reader at the wavelength of 490 nm. All the experiments were repeated three times (n=5). Percentage of adhesion was calculated by using the equation: Adhesion rate (%) = $(A_{treatment\ group}/A_{control\ group}) \times 100$.

Wound-healing assay

Scratch test (wound-healing) assays were performed to evaluate the wound-healing (repair) capability of cells treated with the solvent of DMSO (0.25%) as control, OA and OA-MVLs, respectively. Before experiment, three marked lines were drawn on the outer side of the bottom surface of the 6-well plates in order to take pictures at the same position. Both HepG2 and SMMC-7721 cells were separately collected from culture flasks by trypsinization and centrifugation. The cells were re-suspended in complete medium and adjusted to 5×10^5 cells/mL. Two milliliters of cell suspension was added to each well of 6-well plates and incubated for 24 h at 37°C and 5% CO_2. When the cells reached 90% confluence, the supernatant was removed and cells were wounded by 10 μL pipette tip, followed by washing with PBS for three times to remove cellular debris. The cells were maintained in starvation media containing different concentrations of OA and OA-MVLs (80, 160 and 240 μmol/L), and the wound closure was monitored. The scratch width (SW), distance between the cell fronts on either side of the wound at the same position, was measured and photographed at 0, 24 and 48 h using an inverted microscope and camera (Nikon, Tokyo, Japan). Wound-healing rate or repair rate was estimated according to the formula as: Wound-healing rates (%) = $(SW_{0\,h} - SW_{24\,h\ or\ 48\,h})/SW_{0\,h} \times 100$.

Cell migration and invasion assays in transwell chamber

Transwell plates with 6.5 mm polycarbonate filters and 8.0 μm pore size (Corning Costar, MD, USA) were used in both migration and invasion assays.

For the invasion assay, the transwell insert membranes were pre-coated with 50 μL diluted Matrigel and incubated for at least 4 h at 37°C in a 5% CO_2-humidified atmosphere. Both HepG2 and SMMC-7721 cells were treated with the solvent of DMSO (0.25%) as control, OA and OA-MVLs (80, 160 and 240 μmol/L), respectively. After 24 h incubation, the cells were re-suspended in DMEM with a density of 5×10^5 cells/mL. A total of 200 μL of the cell suspension was added to each upper chamber of a 24-well transwell plate, and 600 μL complete DMEM medium containing 2% FBS as chemo attractant was placed in the lower chamber. The plates were incubated in a 37°C incubator with 5% CO_2 for 24 h. Subsequently, the upper chamber was washed with PBS twice. Then, the cells were fixed in 4% paraformaldehyde for 30 min and stained with 0.1% crystal violet dye for 25 min. After that, the upper chamber was gently washed by PBS three times and the surfaces of the transwell membranes were wiped using cotton swab to remove non-migratory cells. For quantification, the stained cells were counted under a light microscope in five different fields, and the mean number of cells per field was taken to represent the invasive tumor cells. The invasion rate (considering control as 100%) was calculated as $(Cells\ Number_{treatment\ group}/Cells\ Number_{control\ group}) \times 100\%$. At least three chambers from three different experiments were analyzed statistically.

For migration assay, the clear transwell inserts, which were not pre-coated with Matrigel, were used in this experiment. The other procedures were conducted as same as that mentioned in the invasion study.

Statistical analysis

All experiments were repeated at least three times. Values were shown as mean ± standard deviation (SD) and analyzed using GraphPad Prism 5.0 (GraphPad Software, La Jolla, CA, USA). Statistical comparisons between different groups were performed using Student's *t*-test, one-way analysis of variance (ANOVA) or two-way ANOVA. A difference of $P<0.05$ was considered statistically significant.

Results

The optimization and determination for the formulation of OA-MVLs

CCD was performed to optimize the effective factors on the particle size and encapsulation efficiency within a minimum number of experiments. We determined the encapsulation efficiency by HPLC analysis, and the chromatograms of blank MVLs, OA standards and OA-MVLs are shown in Figure 1. The retention time of OA peak in OA-MVLs was consistent with that of standard OA. No interference peaks were observed in the near location of OA peak. The result indicated that this HPLC method developed in this study was sensitive enough to determine OA. In terms of the linearity, the result demonstrated that the standard curve was linear over the range of 5–200 μg/mL with an excellent correlation between peak area and concentration of the drug. The results of the

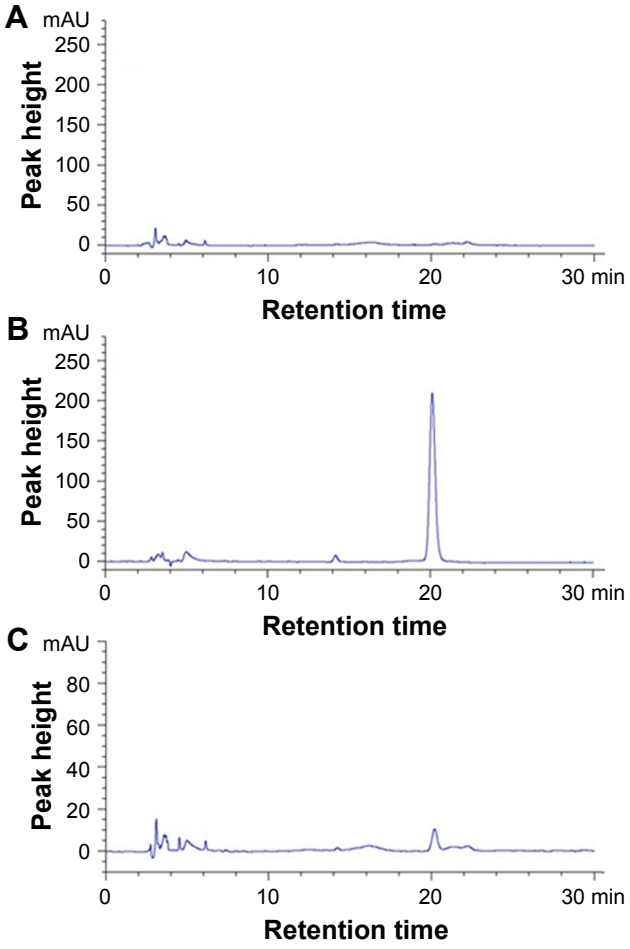

Figure 1 Representative HPLC chromatograms obtained for (**A**) blank MVLs, (**B**) standard OA and (**C**) OA-MVLs.
Abbreviations: HPLC, high-performance liquid chromatography; MVLs, multivesicular liposomes; OA, oleanolic acid.

accuracy and precision demonstrated that the analysis method established in this study showed the intra- and inter-day relative standard deviation (RSD) <10% for these samples. The extraction recoveries of OA at low, medium and high concentration levels were 100.74% (RSD, 0.77%), 100.40% (RSD, 0.79%) and 100.02% (RSD, 0.87%), respectively. All the results suggested that the encapsulation efficiency was reliable under the established analysis method.

Based on the preliminary experiments, the experimental values for individual points (axial star, factor and center) were determined as shown in Table 1. The experimental runs and the observed responses for the 15 formulations are given in Table 2.

Table 1 Independent variables and their levels in coded and physical units

Independent variables	Levels				
	−1.732	−1	0	+1	+1.732
Cholesterol:soybean lecithin (X_1)	0.25	0.36	0.5	0.64	0.75
Total lipids:drug (X_2)	10.00	11.27	13.00	14.73	16.00
Triolein:soybean lecithin (X_3)	0.13	0.25	0.41	0.57	0.69

The regression equations for the responses obtained through the analysis of Statistica 10.0 were as follows:

$$Y_1 = 67.07 + 69.36X_1 + 1.20X_2 + 22.82X_3 - 1.10X_1X_2 + 24.89X_1X_3 + 2.10X_2X_3 - 60.84X_1^2 - 0.053X_2^2 - 92.44X_3^2 \quad (P<0.0001,\ R^2=0.93);$$

$$Y_2 = +0.58 - 7.50X_1 + 1.28X_2 + 63.98X_3 - 81.86X_1X_3 - 5.06X_2X_3 + 22.12X_1^2 + 58X_3^2 \quad (P<0.0003,\ R^2=0.85)$$

These two regression equations represented the quantitative effect of process variables (X_1, X_2 and X_3) and their interactions on their responses Y_1 and Y_2, respectively.

The process was optimized for the responses Y_1 and Y_2 after the polynomial equations relating the dependent and independent variables were generated. The relationship between the dependent and independent variables was further elucidated using response surface and contour plots. The response model was mapped against two experimental factors, while the third was held constant at its middle level (Figure 2). Figure 2A–C and D–F showed the effects of factors (X_1, X_2, and X_3) on the responses Y_1 (encapsulation efficiency) and Y_2 (particle size), respectively. As shown in Figure 2, an optimized formulation (X_1=0.57, X_2=10,

Table 2 Experimental design for three factors and experimental values of objective variables

Run	X_1	X_2	X_3	Y_1	Y_2
1	0.75	13	0.41	93.13	13.43
2	0.64	14.73	0.57	91.67	11.13
3	0.64	14.73	0.25	94.75	9.31
4	0.64	11.27	0.57	90.51	19.40
5	0.64	11.27	0.25	96.10	12.29
6	0.5	16	0.41	95.41	16.45
7	0.5	13	0.69	86.01	26.18
8	0.5	13	0.13	90.61	17.22
9	0.5	10	0.41	94.72	15.45
10	0.36	14.73	0.57	90.00	21.41
11	0.36	14.73	0.25	95.49	12.57
12	0.36	11.27	0.57	87.95	29.29
13	0.36	11.27	0.25	95.59	14.53
14	0.25	13	0.41	90.42	20.40
15	0.5	13	0.41	94.51	11.99
16	0.5	13	0.41	96.99	15.30
17	0.5	13	0.41	96.96	14.90
18	0.5	13	0.41	96.16	14.98
19	0.5	13	0.41	95.72	16.50
20	0.5	13	0.41	96.06	13.21

Notes: X_1, weight ratio of cholesterol/soybean lecithin; X_2, weight ratio of total lipids/drug; X_3, weight ratio of triolein/soybean lecithin; Y_1, encapsulation efficiency (%); Y_2, mean particle size (μm).

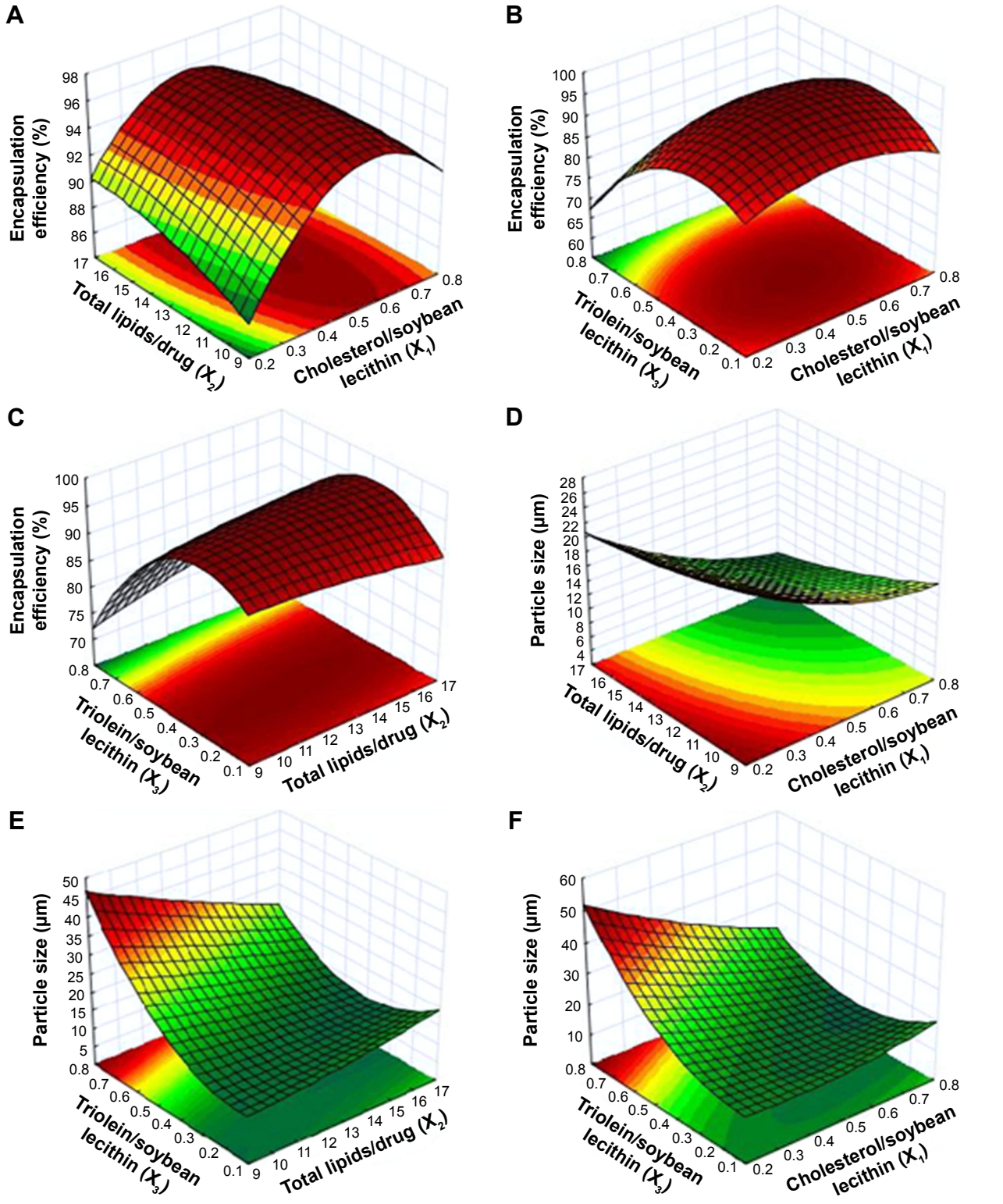

Figure 2 Response surface plot and contour map of the combined effect of (**A**, **D**) X_1 and X_2, (**B**, **F**) X_1 and X_3, and (**C**, **E**) X_2 and X_3 on the encapsulation efficiency (%) and the particle size (μm).

Notes: X_1, weight ratio of cholesterol/soybean lecithin; X_2, weight ratio of total lipids/drug; X_3, weight ratio of triolein/soybean lecithin.

X_3=0.38) was obtained for preparing OA-MVLs with a mean particle size of <20 μm and high encapsulation efficiency. To verify the optimized formulation, OA-MVLs were prepared according to the predicted levels of X_1, X_2 and X_3. As shown in Table 3, obtained Y_1 and Y_2 were in a close agreement with the predicted value. This result demonstrated the reliability of the optimization procedure in predicting the particle size of OA-MVLs and the encapsulation efficiency. Therefore,

Table 3 Comparison of the observed and expected values obtained by constraints applied on Y_1 and Y_2

Variables	Optimized values	Response	Mean values expected	Mean values observed	Bias* (%)
Cholesterol:soybean lecithin (X_1)	0.57	Y_1	95.96	93.19	2.89
Total lipids:drug (X_2)	10				
Triolein:soybean lecithin (X_3)	0.38	Y_2	12.02	11.57	3.75

Notes: Y_1, encapsulation efficiency (%); Y_2, mean particle size (μm). *Bias (%) was calculated as: (*predicted value – observed value*)/*predicted value* ×100 (n=3).

we obtained the optimized formulation from the CCD and RSM, ie, when the amount of OA is 16 mg, the total lipids is in an amount of 156.6 mg (≈160 mg) including soybean lecithin (80 mg), cholesterol (45.6 mg), triolein (30 mg) and stearic acid (1 mg).

OA-MVLs induced cell anti-proliferation

We performed MTT assay to test the effect of OA-MVLs on cell growth inhibition against HepG2, SMMC-7721 and L-02 cells after 24 h treatment. The results shown in Figure 3 indicate that both OA and OA-MVLs show cell proliferation inhibition on the tested cells in a dose-dependent manner within a certain range of concentration. The inhibitory effect of OA and OA-MVLs on L-02 cells was much less than that on the HepG2 and SMMC-7721 cells (Figure 3A), with a half maximal inhibitory concentration (IC_{50}) of 319.45 and 336.09 μmol/L, respectively. At the same concentration of 160 μmol/L, the cell viability of HepG2 and SMMC-7721 cells treated with OA-MVLs is 47.51% and 48.09%, whereas that resulting from OA is 57.08% and 54.95%, respectively (Figure 3B and C). With the treatment of OA and OA-MVLs, the IC_{50} value for HepG2 cells is 198.56

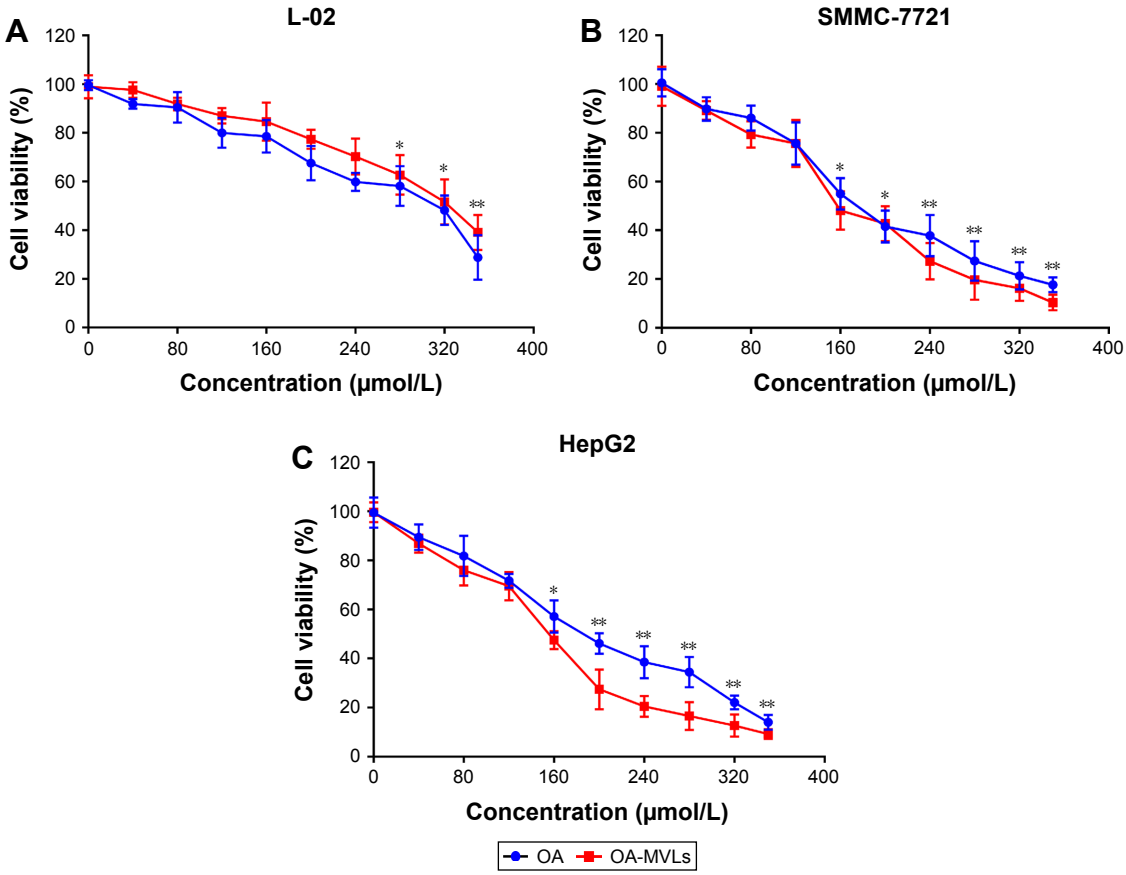

Figure 3 The in vitro cell growth inhibition effect resulted from MTT assay on (**A**) L-02, (**B**) SMMC-7721 and (**C**) HepG2 cells, after being treated separately for 24 h with various concentrations of OA and OA-MVLs.

Notes: The solvent of DMSO (0.25%) was used as vehicle controls. A490 was measured after the MTT incubation. Each data point represents mean ± SD based on five repetitive determinations in three independent experiments. The significance of the differences was evaluated using Student's *t*-test (*$P<0.05$, **$P<0.01$), and the asterisk marks represent the difference of OA vs control and OA-MVLs vs control, respectively.

Abbreviations: MTT, 3-(4,5 dimethylthiazol-2-yl)-2,5-diphenyl-tetrazolium bromide; OA, oleanolic acid; MVLs, multivesicular liposomes; DMSO, dimethyl sulfoxide; SD, standard deviation.

and 160.27 μmol/L, respectively, and the result for SMMC-7721 is 187.36 and 162.50 μmol/L, respectively. This result means that compared to OA, OA-MVLs enhanced the cell proliferation inhibition on both HepG2 and SMMC-7721 cells. Furthermore, the cell viability of blank MVLs on L-02 cells was 95.61%, which implied that blank carrier has no toxic effect on normal liver cells.

OA-MVLs reduce adhesion of HCC cells

With matrix adhesion assay, we found that treatment with both OA and OA-MVLs could significantly inhibit the matrix adhesion of HepG2 and SMMC-7721 cells in Matrigel in a dose-dependent manner (Figure 4), eg, after treatment with OA-MVLs with the concentration increasing from 80 to 240 μmol/L, the number of HepG2 cells adhered to the matrix decreased from 64.48±3.46 to 47.6%±3.12% and that of SMMC-7721 cells also decreased from 67.98±3.98 to 48.95%±6.76% (Figure 4A and B). Meanwhile, Figure 4 showed that with the different concentration treatment at 80, 160 and 240 μmol/L, the adhesion rate of SMMC-7721 cells resulted from OA is 72±6.15, 69.71±3.57 and 68.65%±7.44%, respectively, and that resulted from OA-MVLs is 67.98±3.98, 63.29±5.35 and 48.95%±6.76%, respectively.

For SMMC-7721 cells, there was a significant difference between control group and all OA groups ($P<0.05$), control group and OA-MVLs 160 μmol/L ($P<0.01$), OA 160 μmol/L and OA-MVLs 160 μmol/L ($P<0.01$) and OA 240 μmol/L

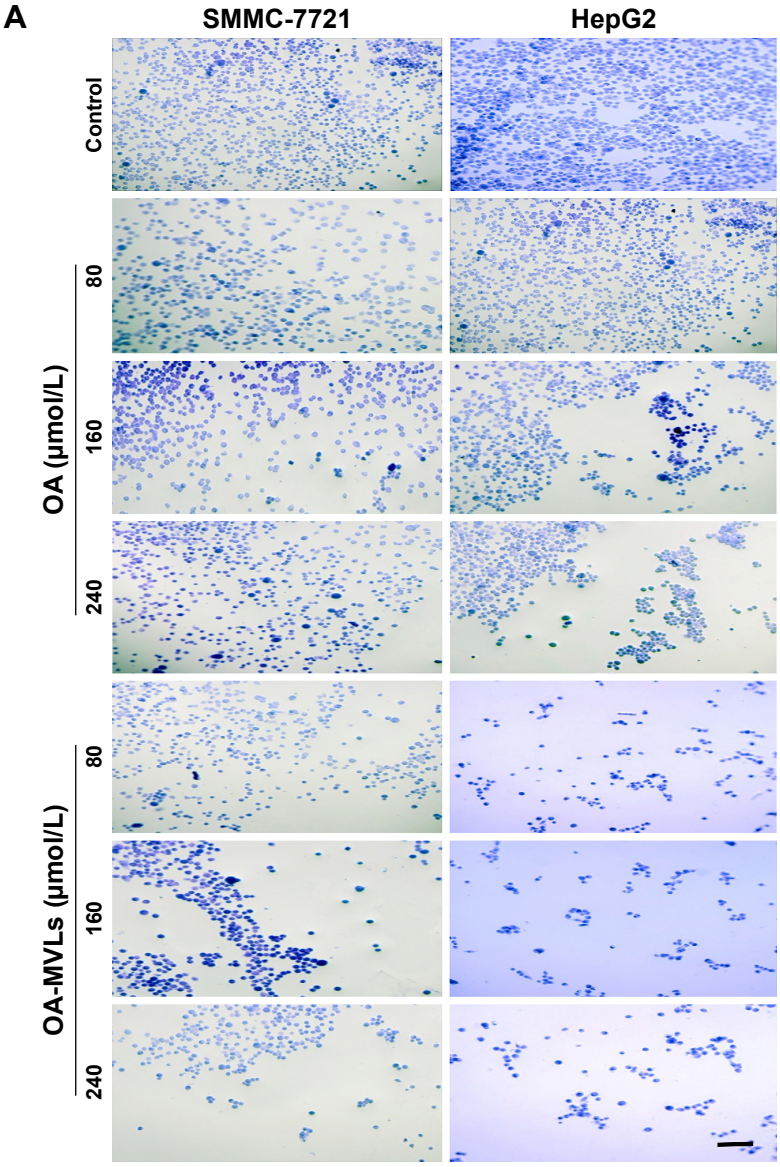

Figure 4 (*Continued*)

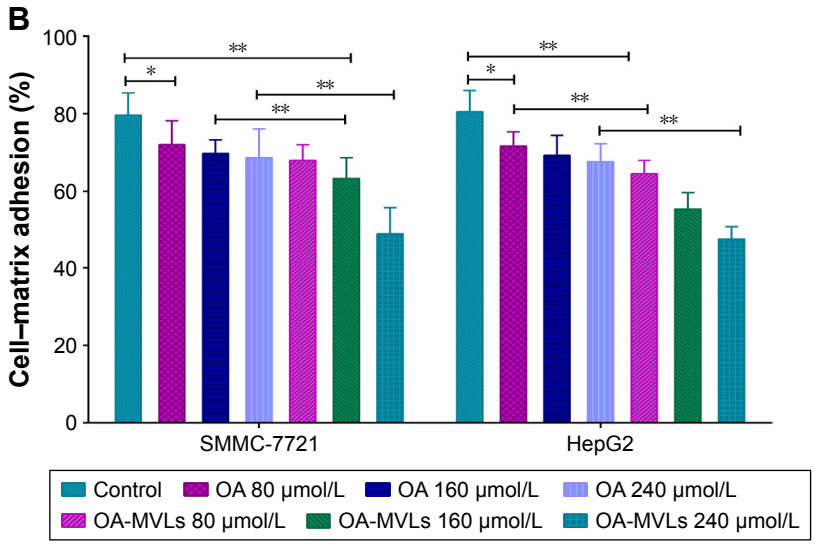

Figure 4 Results of cell–matrix adhesion assays on both SMMC-7721 and HepG2 cells in vitro.
Notes: (**A**) Representative images of SMMC-7721 and HepG2 cells adhered with the Matrigel matrix after treatment with various concentrations of OA and OA-MVLs; (**B**) quantitative analysis of adhesion rate of HepG2 and SMMC-7721 cells detected by MTT assays. Independent experiments were measured in triplicate and repeated at least three times for each cell type. Results are presented as mean ± SD with *$P<0.05$, **$P<0.01$, scale bar 20 μm and magnification (200×).
Abbreviations: OA, oleanolic acid; MVLs, multivesicular liposomes; MTT, 3-(4,5 dimethylthiazol-2-yl)-2,5-diphenyl-tetrazolium bromide; SD, standard deviation.

and OA-MVLs 240 μmol/L ($P<0.01$). On the other hand, for HepG2 cells, there were similar results in difference between control group and each OA group ($P<0.05$), control group and OA-MVLs 80 μmol/L ($P<0.01$), OA 80 μmol/L and OA-MVLs 80 μmol/L ($P<0.01$), OA 160 μmol/L and OA-MVLs 160 μmol/L ($P<0.01$) and OA 240 μmol/L and OA-MVLs 240 μmol/L ($P<0.01$). This result suggested that with a same concentration treatment, OA-MVLs tend to show stronger inhibition effect than OA on matrix adhesion of cancer cells. Moreover, the inhibition effects of OA-MVLs on matrix adhesion of HepG2 and SMMC-7721 cells were similar, indicating that OA-MVLs were able to inhibit different HCC cells.

OA-MVLs suppressed HCC cells migration and invasion in vitro

To explore whether OA-MVLs affect the migratory and invasive capabilities of HCC cells, we performed wound-healing, transwell migration and invasion assays in SMMC-7721 and HepG2 cells that were treated with OA-MVLs and OA at doses of 80, 160 and 240 μmol/L, respectively.

In the result of wound-healing assay (Figure 5), both HepG2 and SMMC-7721 cells treated by control almost fused together at the time point 48 h, but after treatment with OA-MVLs at 80, 160, 240 μmol/L, the repair rate of SMMC-7721cells is 50.08±1.64, 47.41±3.84, and 37.87%±3.97%, respectively, and that of HepG2 cells is 61.89±3.97, 46.69±5.08, and 34.56%±6.45%, respectively. Compared to OA treatment, at the same concentration, OA-MVLs showed stronger inhibition than OA on wound healing of HepG2 and SMMC-7721 cells. This result is consistent with that from the cell growth inhibition analysis by MTT assay.

Meanwhile, the results from the transwell migration and invasion assays were shown in Figure 6. It indicated that the number of migrated and invaded cells significantly decreased in both SMMC-7721 and HepG2 cells treated with OA and OA-MVLs in comparison with that in the control group. For SMMC-7721 cells (Figure 6A and B), after the respective treatment with OA 80, 160 and 240 μmol/L, the migration rate is 81.59±7.68, 60.27±4.59 and 44.17%±6.19%, respectively, and that resulting from OA-MVLs is 63.32±7.74, 41.22±9.63 and 22.43%±6.51%, respectively. Compared with control treatment, OA 160 μmol/L and OA-MVLs 80 μmol/L showed obvious difference ($P<0.05$) and OA 240 μmol/L and OA-MVLs 160 and 240 μmol/L showed significant difference ($P<0.01$). The result of invasion assay is consistent with that of migration test. For HepG2 cells, similar results were shown in Figure 6C and D, in which the migration and invasion rate resulted from OA-MVLs 240 μmol/L is 29.87±2.49 and 21.22%±3.37%, respectively. Meanwhile, both OA and OA-MVLs showed the ability to inhibit cancer cell migration and invasion in a concentration-dependent manner. Moreover, OA-MVLs showed stronger inhibition on both cell migration and invasion than OA at the same concentration. This result is also in agreement with the results from scratch test.

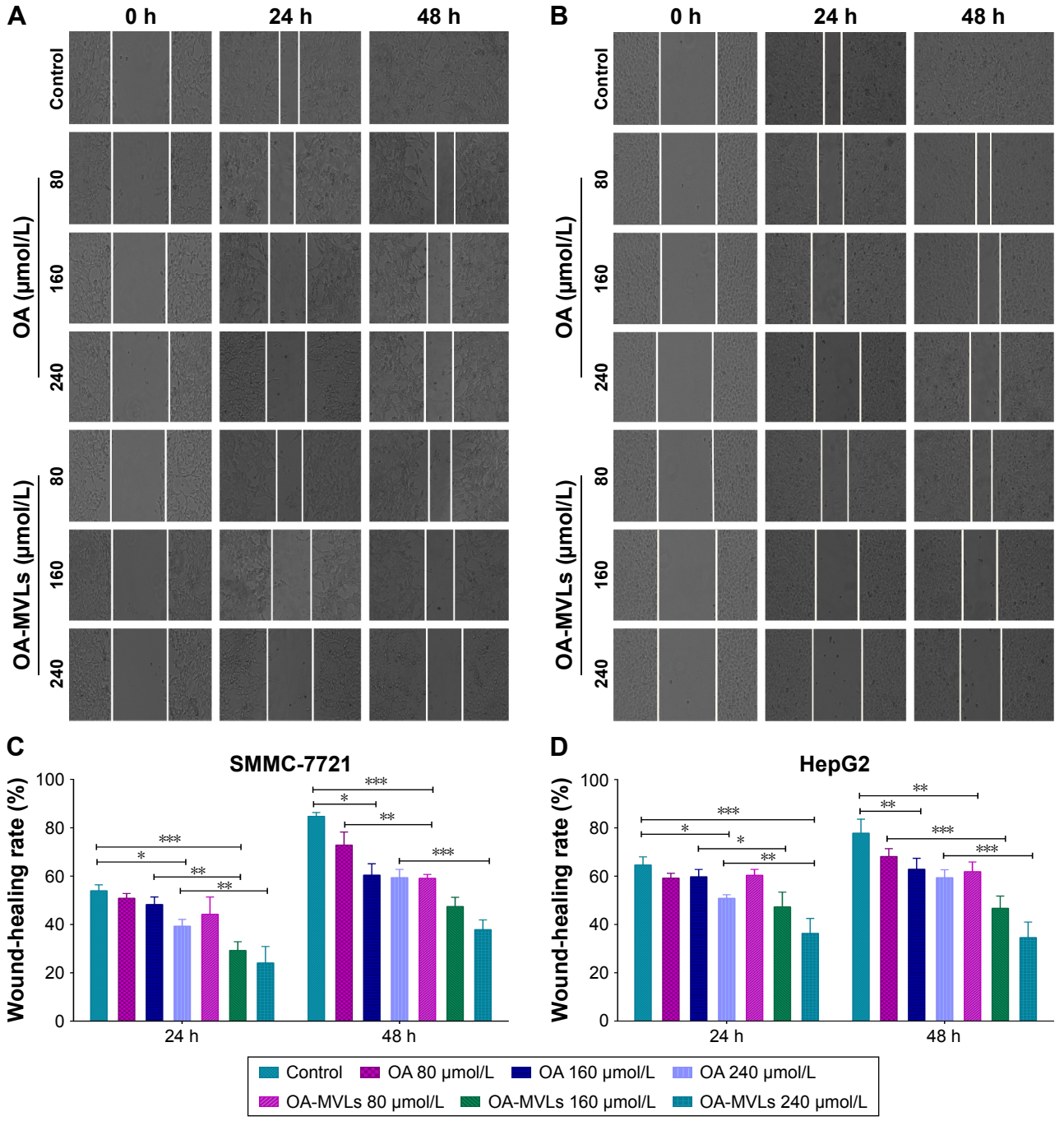

Figure 5 Results from wound-healing assays on SMMC-7721 cells and HepG2 cells.

Notes: Cells were seeded in 6-well plates and incubated overnight. A linear area of attached cells was removed by a pipette tip before treatment with different concentrations of OA and OA-MVLs. (**A**) The SMMC-7721 cells and (**B**) HepG2 cells were photographed at different time points of 0, 24 and 48 h (100×). Meanwhile, the SW, distance between the cell fronts on either side of the wound, was measured. Wound-healing rate of (**C**) SMMC-7721 cells and (**D**) HepG2 cells was estimated according to the formula as: Wound-healing rates (%) = $(SW_{0\,h} - SW_{24\,h\ or\ 48\,h})/SW_{0\,h} \times 100$. Each experiment was performed at least three times; results are presented as mean ± SD with $^{*}P<0.05$, $^{**}P<0.01$ and $^{***}P<0.001$.

Abbreviations: OA, oleanolic acid; MVLs, multivesicular liposomes; SW, scratch width; SD, standard deviation.

In summary, all the earlier results demonstrated that OA and OA-MVLs were able to suppress the migration and invasion abilities of SMMC-7721 and HepG2 cells in a dose- and time-dependent manner in vitro. But OA-MVLs showed a more prominent inhibitory effect than that of OA, indicating that after OA was formulated into MVLs, it could play a better role to inhibit the migration and invasion of cancer cells, which is consistent with our previous research result.[14]

Discussion

As we know, uncontrolled cell proliferation and metastasis are the primordial events of cancer progression. The presence

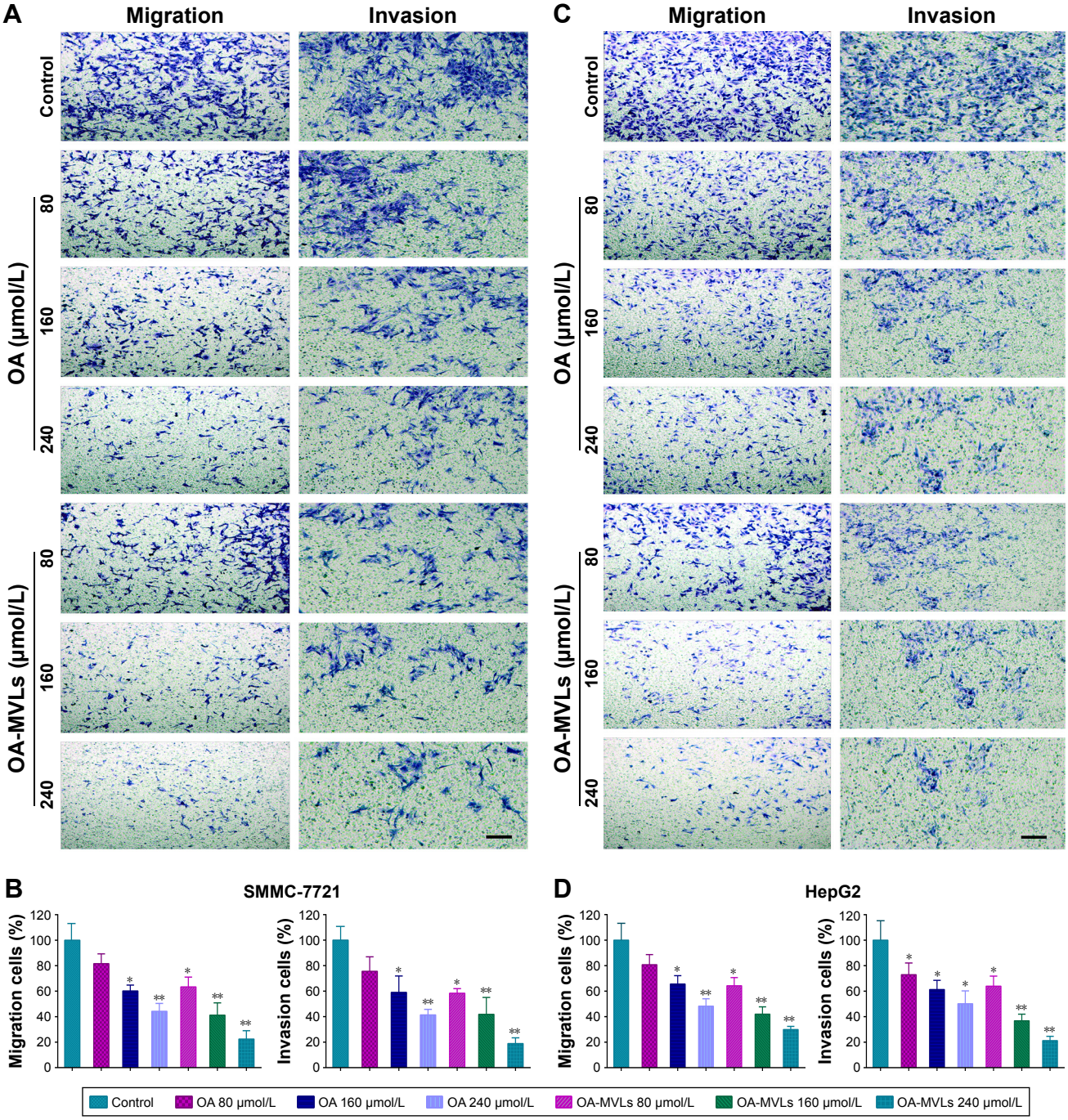

Figure 6 Results from cell migration and invasion assays conducted in transwell chambers.
Notes: After separate treatment with different concentrations of OA and OA-MVLs, the migrated and invaded (**A**) SMMC-7721 cells and (**C**) HepG2 cells stained by crystal violet dye were observed under the light field of microscope. For quantitative analysis, the percent rates of migration and invasion of (**B**) SMMC-7721 cells and (**D**) HepG2 cells were calculated as: ($Cells\ Number_{treatment\ group}$/$Cells\ Number_{control\ group}$) ×100%. At least three chambers from three different experiments were analyzed statistically. Data were shown as mean ± SD with *$P<0.05$ and **$P<0.01$ compared with the control group, magnification (200×) and scale bar (20 μm).
Abbreviations: OA, oleanolic acid; MVLs, multivesicular liposomes; SD, standard deviation.

of metastasis is the main cause of morbidity and mortality in millions of patients with cancer. HCC, like other cancers, is characterized by a multistage process of tumor progression,[19] including invasion of the surrounding tissues, migration and colonization of distant sites in the body, which is a serious public health burden due to poor prognosis and limited therapeutic options. A novel dosage form of MVLs for OA that could effectively retard the growth, migration and invasion of HCC cells would be a potential candidate to suppress cancer progression and metastasis.

In this study, we have developed a novel drug delivery system of OA-MVLs, on the basis of previous experiments,

using CCD with RSM for the performance evaluation of the parameters affecting the particle size and encapsulation efficiency of OA-MVLs to get the optimal formulation. Our laboratory has recently reported that OA-MVLs showed obvious inhibitory effect on HepG2 cells and in order to further verify the inhibition on cancer cell metastasis of the optimized OA-MVLs, we chose both HepG2 and SMMC-7721 cells as the cancer cell model to conduct cytotoxicity assays. The results found that OA-MVLs indeed can effectively reduce the cancer cells vitality of both HepG2 and SMMC-7721 cells and the inhibition effect grew with the increase of the OA-MVLs concentration. Additionally, with the same concentration treatment, OA-MVLs showed similar inhibitory effect on SMMC-7721 cells and HepG2 cells, which implied that OA-MVLs could effectively inhibit different HCC cells. Importantly, OA-MVLs also obviously induced better inhibition effect than that of OA on the liver cancer cells. At the same time, in this study, we also carried out the vitality test of normal liver cells, finding that OA-MVLs have inhibition effect on L-02 cells, but the IC_{50} value in normal cells is much higher than that in HCC cells. When the concentration of OA-MVLs is <160 μmol/L, at 24 h time point, no obvious inhibition effect was observed in normal liver cell vitality, but it could significantly inhibit the growth of liver cancer cells in vitro. To test whether the blank MVLs could have an inhibitory effect on the normal liver cells and cancer cells, we prepared the paralleled formulation of blank MVLs as comparison in all experiments. It turned out that blank MVLs have no inhibition effects on normal liver cells and liver cancer cells.

On the other hand, adhesion is a kind of important physiological processes of cells; the morphology, growth, differentiation, migration and even metabolism of cells are involved with adhesion. However, the most important factor of cancer cell adhesion is the cell-to-cell and cell-to-epimatrix adhesion, with the help of endothelial cells and lymphocyte cells along with the blood and lymph node metastases. Matrix adhesion would promote cancer cells to invade through basement membrane and degrade organizational barriers.[20,21] Therefore, it is important to inhibit cell adhesion to restrain cancer metastasis. Moreover, the impaired cell-to-cell adhesion at the primary site is required for cancer cells to metastasize.[22] Reduced E-cadherin function is the indicator of the loss of cell-to-cell adhesion. In this study, we adopted Matrigel matrix to investigate whether OA-MVLs could suppress the adhesion ability of HCC cells. The results revealed that OA-MVLs were able to reduce adhesion of both HepG2 and SMMC-7721 cells. However, the mechanism about its effect on inhibiting adhesion of HCC cells has not been explored yet. Western blot and pull-down assay should be used to detect whether the effect of OA-MVLs on adhesion in HCC cells is related to E-cadherin.

Invasion and metastasis have been postulated as the "sixth hallmark" of cancer and represent interrelated processes characterized by cell growth, cell adhesion, cell migration and proteolytic degradation of tissue components, including extracellular matrix and basement membrane. In addition, the invasion cells also assist cells to invade the blood vessels or lymphatic and through the circulation of blood to arrive other parts or organs and form the metastases, which is similar to the primary tumor.[23,24] Overexpressed transforming growth factor β1 (TGF-β1) has been demonstrated to be closely relevant to enhanced metastasis in patients with HCC and migratory property of cultured HCC cells.[25,26] Inhibition of TGF-β1 signaling pathway greatly suppressed HCC cell migration.[27] TGF-β1-induced EMT is the key mechanism by which it promoted migration and invasion in liver cancer. Akt activation has been well documented to play a key role in the process of HCC EMT and induced invasion.[28] Recently, myocyte enhancer factor-2 (MEF2) have been verified to act as effectors downstream of Akt pathway during malignant transformation[29] and promote the growth of HCC by accelerating cell cycle progression.[30] Yu et al[11] have reported that OA was able to suppress the invasion and EMT of HCC cells by down-regulating MEF2, showing that targeting this pathway is an effective therapeutic strategy for HCC invasion. Accordingly, in this study, we made MVLs for OA and applied wound-healing, transwell migration and invasion assays to explore whether OA-MVLs also have inhibition effect on HCC cells. Fortunately, consistent with our hypothesis, all the results demonstrated that OA-MVLs were able to suppress the migration and invasion of HCC cells even at a low dose in vitro, which even showed a better effect than OA. However, whether OA-MVLs exhibiting anti-migration activity on HCC is associated with MEF2 should be further investigated.

Collectively, from our experiments, we can conclude that OA-MVLs reduced the proliferation, adhesion, migration and invasion of HCC cells in vitro, which may facilitate the development of therapeutic strategy targeting HCC invasion and metastasis. However, further exploration is necessary to fully understand how OA-MVLs play the role of inhibition, invasion and migration in HCC cells. Some experiments such as immunoblotting assay, quantitative polymerase chain reaction (PCR) and Western blot analysis should be

conducted in future work. Moreover, OA-MVLs should also be investigated for its anti-migration and anti-invasion activity in vivo in further studies.

Conclusion

Taken together, we have applied CCD to optimize the formulation to successfully prepare a novel drug delivery system of OA-MVLs. Then, we designed and performed experiments to prove that OA-MVLs could suppress the ability of HCC cells to adhere, migrate and invade in vitro. Our data indicated that OA-MVLs are a promising agent for HCC cancer therapy and may be used for clinical treatment in the future.

Acknowledgments

Authors would like to thank the following research platforms for their help and support: the Key Laboratory of Medical Electrophysiology of Ministry of Education; Collaborative Innovation Center for Prevention and Treatment of Cardiovascular Disease; the Drug Discovery Research Center; the Department of Medicinal Chemistry School of Pharmacy, Southwest Medical University, Luzhou, Sichuan, China. This work was supported by the General Program of Science and Technology Agency of Sichuan Province (Grant No 2017JY0160); the Collaborative Fund of Luzhou Government and Southwest Medical University (Grant No 2016LZXNYD-J06); the National Natural Science Foundation of China (Grant No 81202479) and the Major Cultivation Item of Educational Department of Sichuan Province (14CZ0018).

Disclosure

The authors report no conflicts of interest in this work.

References

1. Mínguez B, Lachenmayer A. Diagnostic and prognostic molecular markers in hepatocellular carcinoma. *Dis Markers*. 2011;31(3):181–190.
2. Nishida N, Goel A. Genetic and epigenetic signatures in human hepatocellular carcinoma: a systematic review. *Curr Genomics*. 2011; 12(2):130–137.
3. Olsen SK, Brown RS, Siegel AB. Hepatocellular carcinoma: review of current treatment with a focus on targeted molecular therapies. *Therap Adv Gastroenterol*. 2010;3(1):55–66.
4. Ng KK, Lo CM, Liu CL, Poon RT, Chan SC, Fan ST. Survival analysis of patients with transplantable recurrent hepatocellular carcinoma: implications for salvage liver transplant. *Arch Surg*. 2008;143(1):68–74.
5. Liu Y, Zhang JB, Qin Y, et al. PROX1 promotes hepatocellular carcinoma metastasis by way of up-regulating hypoxia inducible factor 1α expression and protein stability. *Hepatology*. 2013;589(2):692–705.
6. Liu J, Wu N, Ma LN, et al. p38 MAPK signaling mediates mitochondrial apoptosis in cancer cells induced by oleanolic acid. *Asian Pac J Cancer Prev*. 2014;15(11):4519–4525.
7. Liu J, Zheng L, Wu N, et al. Oleanolic acid induces metabolic adaptation in cancer cells by activating the AMPactivated protein kinase pathway. *J Agric Food Chem*. 2014;62(24):5528–5537.
8. Liu J, Wu N, Ma L, et al. Oleanolic acid suppresses aerobic glycolysis in cancer cells by switching pyruvate kinase type M isoforms. *PLoS One*. 2014;9(3):e91606.
9. Lúcio KA, Rocha Gda G, Monção-Ribeiro LC, Fernandes J, Takiya CM, Gattass CR. Oleanolic acid initiates apoptosis in non-small cell lung cancer cell lines and reduces metastasis of a B16F10 melanoma model in vivo. *PLoS One*. 2011;6(12):e28596.
10. Hua Y, Zhang Z, Li J, et al. Oleanolic acid derivative DexOA has potent anti-tumor and anti-metastatic activity on osteosarcoma cells in vitro and in vivo. *Invest New Drugs*. 2011;29(2):258–265.
11. Yu W, Huang CS, Wang Q, et al. MEF2 transcription factors promotes EMT and invasiveness of hepatocellular carcinoma through TGF-β1 autoregulation circuitry. *Tumor Biol*. 2014;35(11):10943–10951.
12. Jäger S, Winkler K, Pfüller U, Scheffler A. Solubility studies of oleanolic acid and betulinic acid in aqueous solutions and plant extracts of Viscum album L. *Planta Med*. 2007;73(2):157–162.
13. Jeong DW, Kim YH, Kim HH, et al. Dose-linear pharmacokinetics of oleanolic acid after intravenous and oral administration in rats. *Biopharm Drug Dispos*. 2007;28(2):51–57.
14. Luo YL, Liu ZB, Zhang XQ, et al. Effect of a controlled-release drug delivery system made of oleanolic acid formulated into multivesicular liposomes on hepatocellular carcinoma in vitro and in vivo. *Int J Nanomedicine*. 2016;12(11):3111–3129.
15. Aslan N. Application of response surface methodology and central composite rotatable design for modeling the influence of some operating variables of a multi-gravity separator for coal cleaning. *Fuel*. 2007; 86(5):769–776.
16. Kwak JS. Application of Taguchi and response surface methodologies for geometric error in surface grinding process. *Int J Mach Tool Manuf*. 2005;45(3):327–334.
17. Jain K, Sood S, Gowthamarajan K. Optimization of artemether-loaded NLC for intranasal delivery using central composite design. *Drug Deliv*. 2015;22(7):940–954.
18. Li Y, Cui F, Liu Z, Xu Y, Zhao H. Improvement of xylanase production by Penicillium oxalicum ZH-30 using response surface methodology. *Enzyme Microb Technol*. 2007;40(5):1381–1388.
19. Kanamori H, Kawakami T, Effendi K, et al. Identification by differential tissue proteome analysis of Talin-1 as a novel molecular marker of progression of hepatocellular carcinoma. *Oncology*. 2011;80(5–6): 406–415.
20. Yue L, Cui H, Li C, et al. A polysaccharide from *Agaricus blazei* attenuates tumor cell adhesion via inhibiting E-selectin expression. *Carbohydr Polym*. 2012;88(4):1326–1333.
21. Watson K, Koumangoye R, Thompson P, et al. Fetuin-A triggers the secretion of a novel set of exosomes in detached tumor cells that mediate their adhesion and spreading. *FEBS Lett*. 2012;586(19):3458–3463.
22. White CD, Brown MD, Sacks DB. IQGAPs in cancer: a family of scaffold proteins underlying tumorigenesis. *FEBS Lett*. 2009; 583(12):1817–1824.
23. Carey SP, D'Alfonso TM, Shin SJ, Reinhart-King CA. Mechanobiology of tumor invasion: engineering meets oncology. *Crit Rev Oncol Hematol*. 2012;83(2):170–183.
24. Perlikos F, Harrington KJ, Syrigos KN. Key molecular mechanisms in lung cancer invasion and metastasis: a comprehensive review. *Crit Rev Oncol Hematol*. 2013;87(1):1–11.
25. Lee D, Chung YH, Kim JA, et al. Transforming growth factor beta 1 overexpression is closely related to invasiveness of hepatocellular carcinoma. *Oncology*. 2012;82(1):11–18.
26. Xu Z, Shen MX, Ma DZ, Wang LY, Zha XL. TGF-beta1-promoted epithelial-to-mesenchymal transformation and cell adhesion contribute to TGF-beta1-enhanced cell migration in SMMC-7721 cells. *Cell Res*. 2003;13(5):343–350.
27. Fransvea E, Mazzocca A, Santamato A, Azzariti A, Antonaci S, Giannelli G. Kinase activation profile associated with TGF-betadependent migration of HCC cells: a preclinical study. *Cancer Chemother Pharmacol*. 2011;68(1):79–86.

28. Hu G, Wei Y, Kang Y. The multifaceted role of MTDH/AEG-1 in cancer progression. *Clin Cancer Res*. 2009;15(18):5615–5620.
29. Di Giorgio E, Clocchiatti A, Piccinin S, et al. MEF2 is a converging hub for histone deacetylase 4 and phosphatidylinositol 3-kinase/Akt-induced transformation. *Mol Cell Biol*. 2013;33(22):4473–4491.
30. Ma L, Liu J, Liu L, et al. Overexpression of the transcription factor MEF2D in hepatocellular carcinoma sustains malignant character by suppressing G2-M transition genes. *Cancer Res*. 2014;74(5):1452–1462.